

# **The RHIC Experimental Program: Highlights from the first year of operation**

Jim Thomas

Lawrence Berkeley National Laboratory, Berkeley, CA

## **Introduction:**

The Relativistic Heavy Ion Collider (RHIC) is located at Brookhaven National Laboratory on Long Island, New York. The collider is 3.83 km in circumference and it accelerates a variety of heavy ion beams; from protons to gold. The top energy is 250 GeV per beam for protons and 100 GeV/amu per beam for gold. So, the collision energies are  $\sqrt{s} = 500$  GeV and  $\sqrt{s} = 200$  GeV/amu, respectively. The design luminosity for heavy ions is  $2 \times 10^{26} \text{ cm}^{-2} \text{ sec}^{-1}$  and the beam lifetime will eventually be greater than 10 hours. RHIC is also capable of running polarized protons and it will have a full complement of Siberian Snakes. The detectors have been designed to measure scattering asymmetries and so a robust program of polarized physics will be possible, in the future.

RHIC has completed two run cycles. The first run ended in 2000 and the second run ended in 2002. Au+Au beams were run at  $\sqrt{s} = 130$  GeV/amu for the first cycle and then the beam energy was raised to  $\sqrt{s} = 200$  GeV/amu for the second cycle of operation. There was also a brief p+p run at 200 GeV in 2002 to test the capabilities of the polarized beam facilities. I will report on the physics results that have been achieved with the heavy ion data in the 2000 run.

The motivation for building RHIC was to study nuclear matter under extreme conditions, at high temperature, and at densities greater than 10 times normal nuclear matter density. Under these conditions, we expect quark and gluon degrees of freedom to become important and the underlying dynamics should change as the nuclear system makes the transition from cold matter to extremely hot and dense matter. In fact, it was predicted that nuclear matter will undergo a phase transition into a Quark Gluon Plasma (QGP) at a critical temperature near the rest mass of the pion and at about 10 times the density of normal nuclear matter. This prediction has been explored with lattice gauge calculations and these calculations have routinely shown that there is a large jump in the energy density for two and three flavor systems at a critical temperature,  $T_c$ , of 160 MeV<sup>1</sup>; see Figure 1. The lattice calculations have a difficult time dealing with the mass of quarks as they appear in nature and so we do not know if the phase transition is first order, second order, or whether there is a tri-critical point on the phase diagram. So, experimentally we are hoping to learn more about hot, dense, matter and to see if nuclear systems undergo a first or second order phase transition into a QGP or perhaps a cross over from one side of the diagram to the other without exhibiting any critical behavior at the cross-over point.

## **The Detectors:**

Four experiments took data in the 2000 run cycle. They are STAR<sup>2</sup>, PHENIX<sup>3</sup>, BRAHMS<sup>4</sup> and PHOBOS<sup>5</sup>. STAR and PHENIX are the large experiments and PHOBOS and BRAHMS are smaller experiments; each with a more specialized physics agenda.

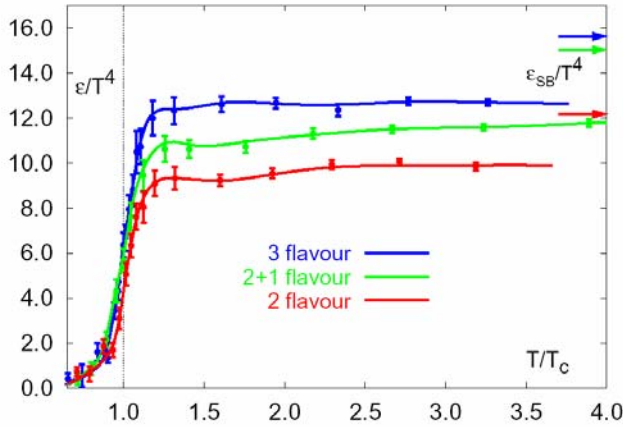


Figure 1: Lattice gauge calculation of the energy density in a system of quarks with 2 or 3 flavors. The figure is from reference 1. The arrows on the right hand side of the figure indicate the Stephan Boltzman limit for a free Quark Gluon gas.

STAR is the hadronic signals experiment. It uses the world's largest time projection chamber (TPC) as its primary tracking detector<sup>6</sup>. See Figure 2. The TPC is 4.2 meters long and 4 meters in diameter. It has full azimuthal coverage and records tracks in the range from  $-1.8$  units to  $1.8$  units of rapidity and it sits in a solenoidal magnetic field of 0.5 Tesla. Charged particle tracking close to the interaction region is accomplished by a Silicon Vertex Tracker (SVT) consisting of 216 silicon drift detectors arranged in 3 layers. The TPC and SVT allow for identification of secondary vertices from weak decays of, for example,  $\Lambda$ ,  $\Xi$ , and  $\Omega$ 's. For the 2000 and 2002 runs, the TPC was supplemented by a ring imaging cherenkov detector to extend the particle ID to high transverse momentum. And in the future, STAR will have a full barrel calorimeter, and additional detectors. Only the TPC and the RICH were operational in the 2000 run.

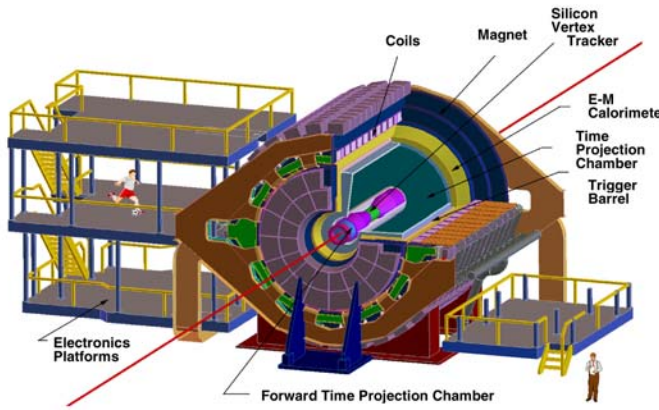


Figure 2: The STAR experiment measures hadronic observables using a large acceptance Time Projection Chamber, a Silicon Vertex Tracker, a Ring Imaging Cherenkov Detector and other detectors. In the future, STAR will have a full barrel Electromagnetic Calorimeter.

PHENIX is a multi-purpose experiment that includes central rapidity hadron and electron spectrometers as well as muon arms at forward rapidities. See Figure 3. The central arms each cover 90 degrees in  $\phi$  and they cover the range from  $-0.35$  units to  $0.35$  units of rapidity. The central arms include tracking chambers and a time of flight wall (TOF) for charged particle measurements plus a RICH backed up with calorimeters for electron, photon and neutral particle energy measurements. In the future, PHENIX will have forward and backward facing muon spectrometers which will provide excellent tracking and particle ID for muons in the range from 1.1 to 2.5 units of rapidity. Only the central arm spectrometers were operational in the 2000 run.

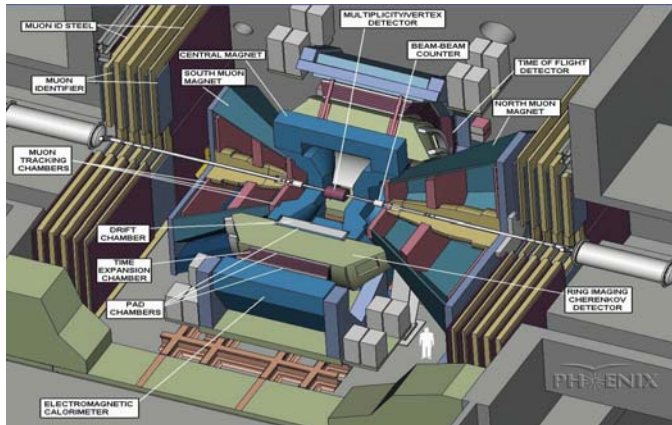


Figure 3: The PHENIX experiment measures leptons, photons and hadrons in selected solid angles using tracking chambers, EM Calorimeters, and Ring Imaging Cherenkov detectors. In the future, PHENIX will have muon arms in the forward and backward directions. The figure is provided courtesy of the PHENIX collaboration.

The BRAHMS experiment has two spectrometers. Each arm is designed to be versatile and to cover a wide rapidity interval, albeit with a small aperture. The arms rotate about a common axis and the mid-rapidity spectrometer covers the angular range from 95 to 30 degrees. The Forward spectrometer extends this coverage from 30 degrees to 2.3 degrees with respect to the beam. This allows BRAHMS to achieve the widest rapidity coverage of all the experiments at RHIC; from  $0 < \eta < 4$ . See Figure 4.

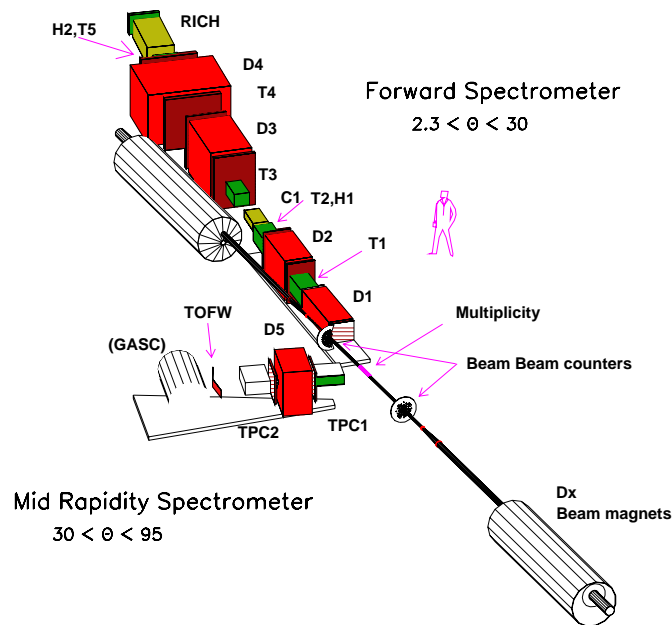


Figure 4: The BRAHMS experiment measures inclusive hadronic particle production over a large rapidity and a large  $p_t$  range. It uses two moving spectrometer arms. The figure is provided courtesy of the BRAHMS collaboration.

The PHOBOS experiment is a table-top two arm spectrometer. It includes a strong field magnet with many layers of Silicon micro-strip detectors surrounding the strong field region to do the spectroscopy of low  $p_t$  charged hadrons. It also has additional silicon detectors to measure charged particle multiplicities into  $4\pi$  solid angle and two time-of-flight walls (TOF) to improve the particle identification capabilities in specific rapidity intervals. See Figure 5.

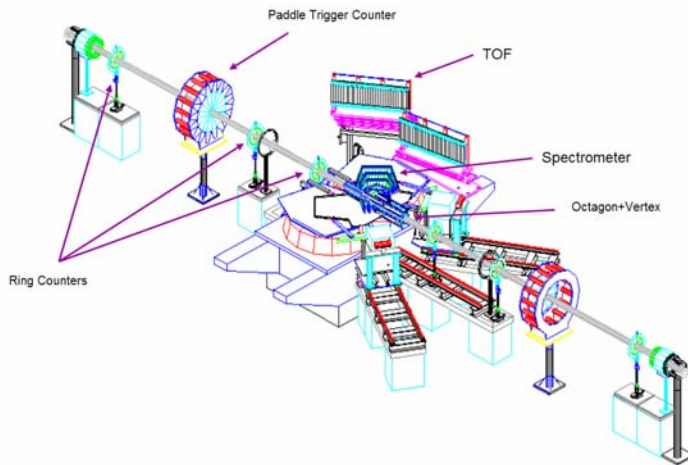


Figure 5: The PHOBOS experiment measures low  $p_t$  charged hadrons into  $4\pi$  azimuth. The figure is provided courtesy of the PHOBOS collaboration.

Finally, there are a set of zero degree calorimeters<sup>7</sup> (ZCALs) installed in all four experiments and they are used to classify the events seen by each experiment. They are located  $\pm 17$  meters from the interaction vertex and they are located behind the first bend magnet in each beamline. The primary purpose of the the ZCALs is to collect the neutral particles that are moving in the forward and backward directions. The response of the ZCALs is non-linear because there is an abundance of neutral particles in mid-peripheral collisions but a deficit in very peripheral collisions, due to a lack of interacting particles, and a deficit in central collisions because the colliding nuclei have evaporated. Therefore, the ZCAL response is not unique and charge particle multiplicity counters are used to break the ambiguity. See Figure 6.

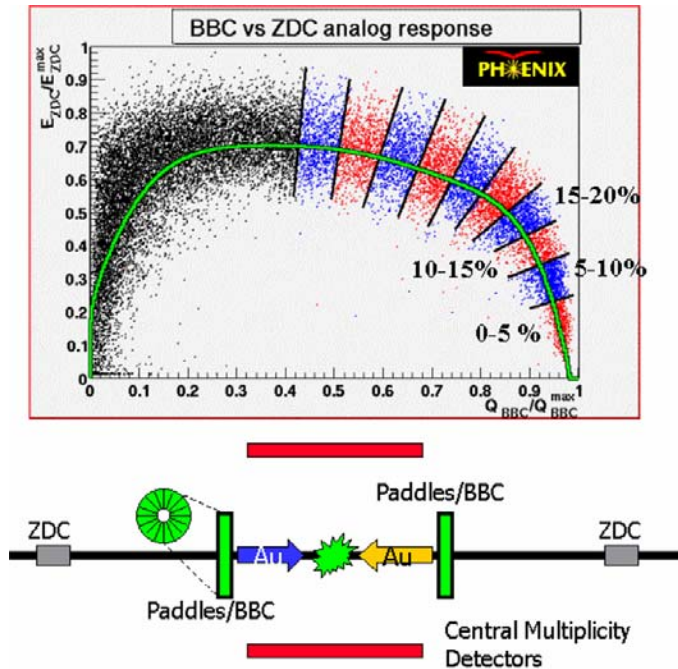


Figure 6: The Zero Degree Calorimeters measure neutrons moving in the forward and backward directions. The ZDC response is double-valued because the mid-peripheral collisions yield a large number of beam-like neutrons but peripheral collisions yield very few neutrons and central collisions also yield very few beam-like neutrons. The labels identify the top 5% of the interaction cross-section, top 10%, and so forth. The figure is provided courtesy of the PHENIX collaboration.



The ZCALs provide a common triggering and analysis tool for each experiment. Thus, it is possible to quantitatively compare data from all four experiments according to whether the data came from the most central collisions (e.g. top 5% of the interaction cross-section) or from more peripheral collisions.

But perhaps the most satisfying part of the detector program is that they work. The first events were recorded by the STAR collaboration on June 25<sup>th</sup>, 2000 and all four detectors observed Au-Au collisions during the first run of the RHIC accelerator. A beautiful example of an event as seen in the STAR TPC, and displayed by the online level three trigger, is shown in Figure 7.

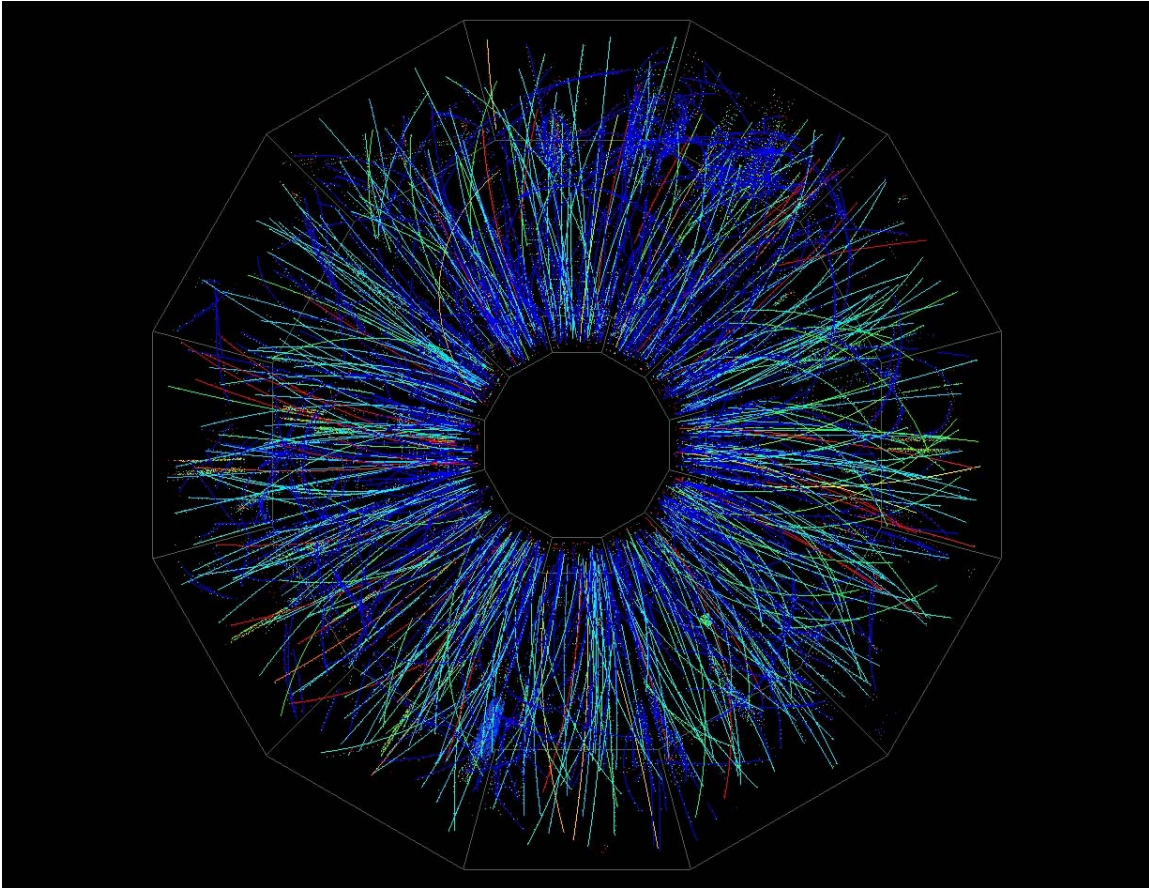


Figure 7: A low multiplicity event seen in the STAR TPC. The beam line goes into the page and through the center of the figure. The colors represent different rates of energy loss for each track.

Figure 7 is an end-view of an event seen in the STAR TPC. The detector is azimuthally symmetric and it has an active volume starting at 50 cm from the beam axis and extending to 200 cm from the beam axis. This is a low multiplicity event, which was chosen so you can see the individual tracks in a projected view. However, event multiplicities up to several thousand per unity rapidity are routinely seen, recorded, and analyzed by the TPC.

## Physics Results from the First Year of Operation at RHIC:

The RHIC experimental program finished its first cycle of operation in September, 2000, and its second cycle of operation in January, 2002. I will concentrate on published data from the first cycle of operation because the data from the second cycle has not been fully analyzed yet ... with one exception. The PHOBOS collaboration has measured the multiplicity of particles produced in RHIC collisions at 56, 130, and 200 GeV per nucleon<sup>8,9</sup>. The 56 and 130 GeV data were taken during the first cycle of operation while the 200 GeV data point is a very fast analysis that was done with data taken in the 2<sup>nd</sup> cycle of operation.

Figure 8 shows the PHOBOS data in comparison to the HiJing model<sup>10</sup>. The multiplicity of charged particles, scaled by the number of participating nucleons ( $N_{\text{part}}$ ), is shown versus the number of participating nucleons. The data are interesting because the maximum multiplicities at RHIC are large but not as large as expected from simple ideas about a first order phase transition. Naive extrapolations, made before these data were available, suggested that a first order jump from 3 pionic degrees of freedom to 37 gluonic degrees of freedom in a QGP would lead to a huge increase in particle production in the final state. Clearly, this does not happen at 130 or 200 GeV. But rather than suggest that we have not seen the QGP, the data are telling us that hot and dense matter produced in RHIC collisions is more complex than we had anticipated. Many models and many predictions were made before the data were available and almost all of them fail to describe the data. The HiJing model is the rare exception. It was available before the data were taken and, at least, it is a good description of particle multiplicities at RHIC. The interesting thing about HiJing is that it was created as a description of hard processes in nuclear collisions, such as jets and mini-jets, and it was not tuned to, and is not a good description of, the soft physics that is dominant at lower energies and yet is still important at RHIC; especially during the final state hadronization phase.

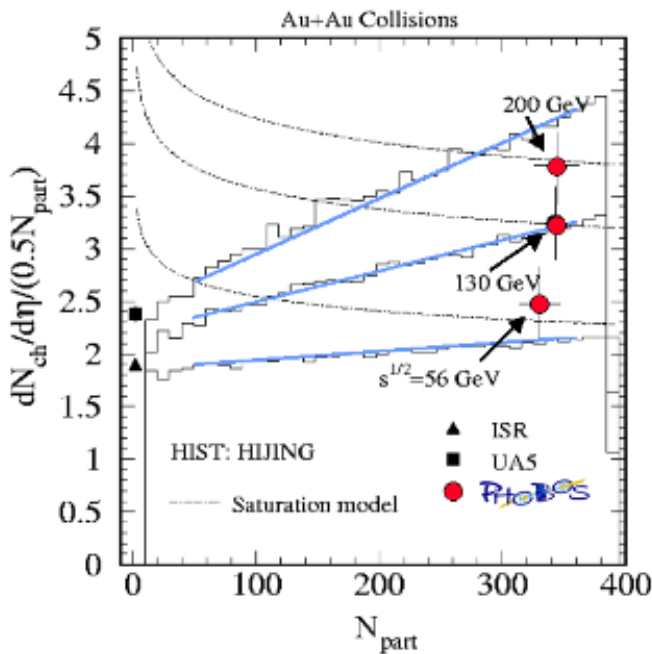


Figure 8: The PHOBOS collaboration made the first measurements of maximum multiplicities at RHIC. The multiplicities are large but not as large as expected. The figure is from Ref. 10 but it has been modified to include the 200 GeV data point from Ref. 9. The HiJing calculations are shown as a histogram with a solid line to guide your eye.

The BRAHMS collaboration has data that can extend our comparison of the data and theoretical models in very interesting ways because their spectrometer can be rotated through a wide range of laboratory angles. Thus, they can collect data over a very broad rapidity interval. See Figure 9. The figure and the data are from reference 11, while the model calculations are from references 10, 12, and 13.

UrQMD<sup>12</sup> is an elegant example of a model that was built to simulate ultra-relativistic heavy ion collisions. It follows the course of a reaction, collision by collision, and it was built using a set of known physical processes and cross-sections. So it is a surprise to find that while UrQMD does an excellent job of simulating final state hadronization, it is not a good description of RHIC multiplicity data. See Figure 9.

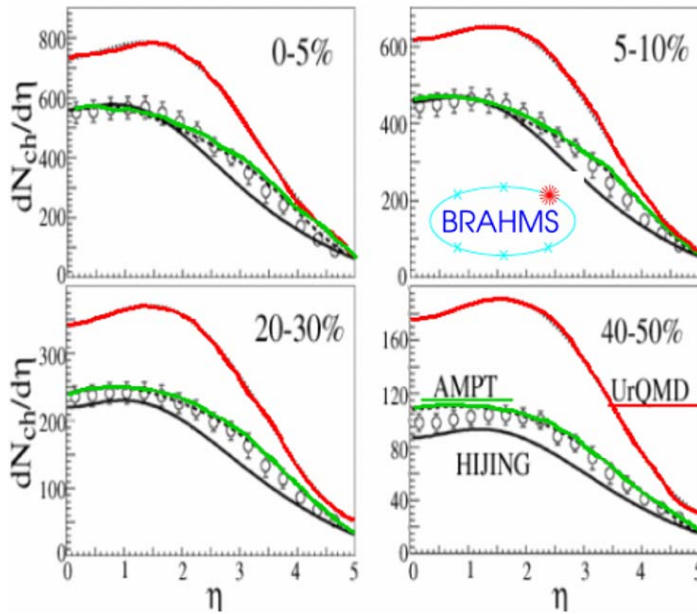


Figure 9: The BRAHMS collaboration has made charged particle multiplicity measurements over a very wide rapidity interval. The data help discriminate between models which are used to describe heavy ion collisions.

The AMPT model<sup>13</sup> is built upon the initial parton momentum distributions generated by the HIJING model and then it adds its own unique hadronization scheme in the final state. This leads to modifications of the HiJing predictions which are generally supported by the data. Another important observation from the BRAHMS data shown in Figure 9 is that the multiplicity of particles is invariant with respect to pseudo-rapidity over an interval of about 2 units. It is not invariant over the full range of RHIC multiplicities. Thus, the simple idea of a Bjorken tube in which hadronization is invariant is an approximation that is not fully born out by the data. This behavior can also be seen in the BRAHMS  $p$ -bar to  $p$  ratios<sup>14</sup> as a function of rapidity. Here too, the ratio is not constant but falls off after 1.5 units of pseudo-rapidity. This indicates that hadronization and baryon production is not invariant across pseudo-rapidity as suggested by a simple Bjorken model.

So, it is clear that the PHOBOS and BRAHMS data discard a wide class of models that were expected to be a good description of the data and, in particular, models based on soft processes at lower energies appear to be inaccurate at RHIC energies. Instead, hard processes such as mini-jet production are beginning to play an important role. In

addition, final state interactions seem to be scaling according to the initial state gluon densities.

Kharzeev and Nardi<sup>15</sup> have started to explore this idea. They propose a simple separation of hard and soft processes according to whether the observed process scales as the number of participating nucleons in a collision (soft process) or the number of binary collisions (hard process). In the perturbative picture, the “hard” component of multiplicity is proportional to the mini-jet production cross section.

$$\frac{dN_{ch}}{d\eta} = (1-x) \frac{N_{pp}}{2} \langle N_{part} \rangle + x N_{pp} \langle N_{coll} \rangle \quad (1)$$

The PHOBOS collaboration has fit their multiplicity data<sup>16</sup> with this equation and they find that the hard process coefficient is  $x \approx 0.15$ . This simple scaling rule for soft and hard processes quantifies how important the hard processes are in the production of charged particle multiplicity. This result is incompatible with final state saturation models but it is consistent with initial state gluon saturation models.

Kharzeev and Levin<sup>17</sup> have used an initial state gluon saturation model to predict the total charged particle multiplicity and the rapidity dependence of charged particle production at 200 GeV before it was measured. They predicted an increase of 10-14% between 130 and 200 GeV and PHOBOS measured  $14 \pm 6\%$ . The Kharzeev and Nardi prediction is based on the RHIC 130 GeV data as well as CERN and HERA data at lower energies. The essential idea behind their calculations is that particle multiplicities are proportional to the number of gluons in the initial state. But the initial state in ultra-relativistic heavy ion reactions is Lorentz contracted and the low momentum gluons interact coherently with the entire Nucleus. The running of the coupling constant ensures that the coupling is large for the low momentum gluons and thus the cross-section for combining low momentum gluons into higher momentum gluons is large ... so large that the initial state is saturated and  $\rho\sigma = 1$ . ( $\rho$  is the density of gluons and  $\sigma$  is the cross-section for glue-gluon interactions.) The saturation condition reduces the flux of low momentum gluons and reduces the multiplicity of particles in the final state relative to what you might expect from a simple extrapolation of gluon number based on the increase in  $\sqrt{s}$ . This explains, in part, why the early models of RHIC collisions were wrong. They did not correctly include the suppression of particle yield due to gluon saturation in the initial state. Thus, the data suggest that final state particle multiplicities depend on the properties of the initial state in ways that we did not expect.

RHIC data are full of surprises. The Lorentz properties of the initial state are important. We haven't found any evidence for a simple first order phase transition from ordinary hadronic matter to a quark gluon plasma; and the final state particle multiplicities are lower than we expected. So the early ideas that were used to motivate the program are showing their humble origins. However, we have discovered some things that are unusual and which cannot be fully explained. Flow is an example; both radial and elliptic flow.



Radial flow is a measure of the collective motion of particles away from their point of interaction while elliptic flow is a measure of the asymmetry of this particle distribution in momentum space.

The radial expansion of the fireball, created during a nucleus-nucleus collision, has thermal characteristics and so a plot of the differential multiplicity versus the transverse mass,  $m_T$ , is exponential. The inverse slope of the exponential is loosely referred to as the temperature, however, the temperature is different for different particle species and strongly dependent on the particle mass. Xu<sup>18</sup> has proposed that the mass dependence has a simple explanation because the total kinetic energy of a particle has two components; a thermal component and a kinematical component.

$$\bar{E} = \frac{3}{2}T + \frac{1}{2}mv^2 \quad (2)$$

Using equation 2, Xu proposed a universal freeze out temperature that is common to all particle species once the mass dependent kinematical term is removed from the data. Xu and Kaneta<sup>19</sup> have performed this analysis for pion, kaon, and proton spectra that were measured by the STAR collaboration. They find that there is a well defined freeze-out temperature at RHIC and it is  $120 \pm 15$  MeV. The data also suggests that the average radial flow velocity,  $\beta$ , of these particles is  $0.55 \pm 0.1$  c at  $\sqrt{s} = 130$  GeV. This is very surprising. The freeze-out temperatures at RHIC are essentially the same as at CERN and the AGS while the radial expansion velocity at RHIC (130 GeV) is a substantial increase over the CERN and AGS values. See Figure 10.

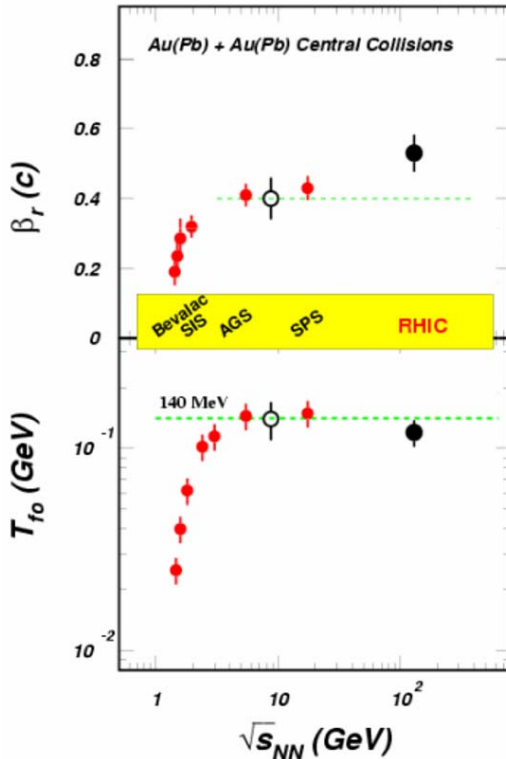


Figure 10: Radial flow measurements suggest explosive radial expansion and high pressure in nuclear collisions at RHIC. For example, the radial expansion velocity is 55% of the speed of light at 130 GeV and it is apparently climbing with  $\sqrt{s}$ . On the other hand, the freeze out temperature is saturated and does not appear to be climbing with  $\sqrt{s}$ .

Now let's turn to elliptic flow. Elliptic flow is a measure of the asymmetry of the emission pattern of particles in momentum space following a peripheral nucleus-nucleus collision. It is the result of the almond shaped overlap zone between two nuclei when they collide, and the flow value is a measure of the efficiency with which this coordinate space asymmetry can be translated into momentum space. One consequence of the geometric asymmetry in the overlap zone is that it is easiest for particles from the center of the collision to emerge along the short axis of the almond. Or, equivalently, one can think of the surfaces of the almond as emitters of particles and there is more surface area facing to the side than to the top (if the long axis of the almond is vertical). Either thought leads to the idea that a coordinate space asymmetry can be translated into a momentum space asymmetry in the emission of particles after a heavy ion collision. It is traditional to perform a Fourier decomposition of the momentum space particle distributions in the x-y plane and  $v_2$  is the coefficient of the 2<sup>nd</sup> harmonic term. In other words:

$$v_2 = \langle \cos(2\phi) \rangle \quad \text{where} \quad \phi = \arctan\left(\frac{p_y}{p_x}\right) \quad (3)$$

and  $p_x$  and  $p_y$  are the momenta of the individual particles. The average is performed over all particles in the event. The RHIC data show that  $v_2$  is large at  $\sqrt{s} = 130$  GeV. The peak value, integrated over all  $p_T$ , is 6% for peripheral collisions<sup>20</sup>. The same quantity measured at the AGS is 2% and the value measured at the SPS is 3.5%. Hydrodynamical models predict that elliptic flow will always be large and these models consistently over-predict the amount of flow at lower energies but they seem to get it right at RHIC energies. See Figure 11. In contrast, Cascade models such as UrQMD successfully predict the amount of flow observed at the SPS but they fail to predict the amount of flow at RHIC.

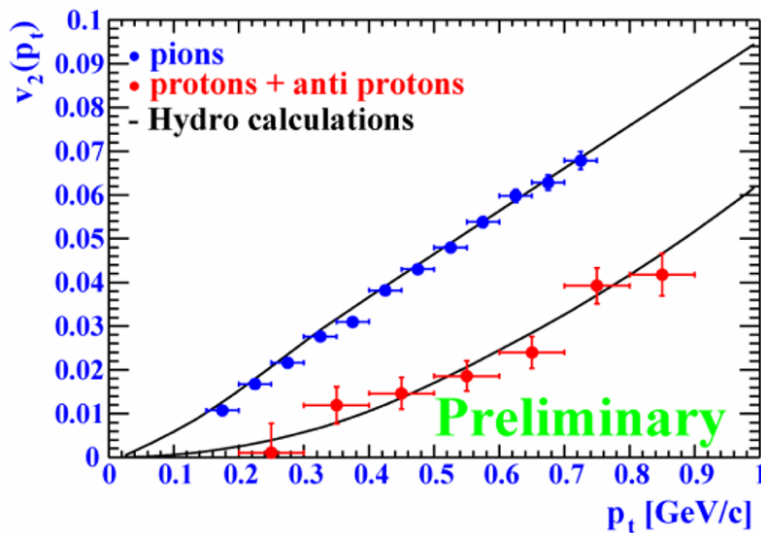


Figure 11: Elliptical flow is large at RHIC and the mass dependence of the signal is in good agreement with hydrodynamical calculations. These data are from the STAR collaboration<sup>21</sup>. Pion and proton data are shown. The solid lines are the predictions of a hydro-dynamical model (modified blast wave).

$v_2$  as a function of  $p_T$  is shown in Figure 11<sup>21</sup>. The interesting feature in Figure 11 is that flow increases with  $p_T$  as predicted by hydrodynamics and the model does a good job of describing the mass dependence of the data. This is a surprise because hydrodynamics assumes thermal equilibrium and therefore the data is suggesting that the system evolves very rapidly towards an equilibrium state; much more rapidly than at the SPS and more rapidly than was anticipated for RHIC.

The hydrodynamical model predicts that flow persists to very high transverse momentum. However, the data do not support this prediction. The data<sup>22,23</sup> show a pronounced saturation effect and the amount of elliptic flow levels off at momenta above 2 GeV/c. See Figure 12. The data suggest that the process which generates flow is being attenuated at high  $p_T$  and some kind of quenching is going on in the fire ball. This is a surprise and was not anticipated at RHIC.

The initial attempts at describing the data with a cascade model required unreasonably high initial gluon densities or extreme elastic parton cross-sections. More recently, Gyulassy, Vitev, and Wang<sup>24</sup> have approximately reproduced the data by dividing the problem into a soft non-perturbative component, which includes hydrodynamic elliptic flow, and a perturbative QCD hard component. The hard component includes jet quenching and energy loss that is a function of the initial gluon density achieved in the collision. See Figure 12.

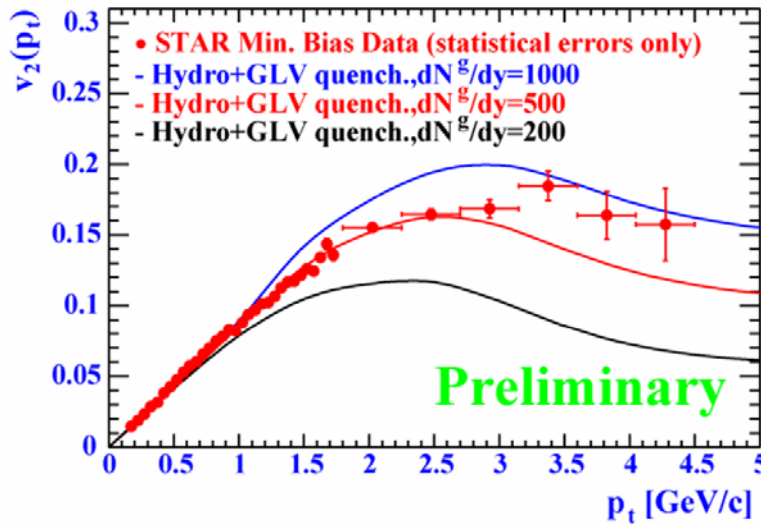


Figure 12: The elliptical flow signal for pions persists to high momentum and saturates above 2 GeV/c. These data, from the STAR collaboration, suggest that the flow signal is preferentially quenched at high  $p_T$ .

A related phenomena can be seen by comparing A-A and p-p scattering cross-sections at high  $p_T$ . The cross-section for scattering Au on Au is a steeply falling exponential function. Similarly, the cross-section for scattering protons on protons is a steeply falling exponential function and so we might expect that the Au-Au cross-section is a simple super-position of p-p interactions. For example, the ratio between the Au-Au cross-section and the p-p cross-section at low  $p_T$  should be proportional to the number of wounded nucleons in the collision<sup>25</sup>, and the ratio at high  $p_T$  should be proportional to the

number of binary encounters in the collision. In between these two limits, we should see a smooth transition from soft to hard physics.

Figure 13 shows the ratio of inclusive spectra for charged hadrons at 130 GeV compared to the UA1 p-p-bar spectrum interpolated to 130 GeV<sup>23</sup>. The binary collision limit and the wounded nucleon limit are shown on the figure. The interesting feature is that the ratio does not rise from the wounded nucleon scaling limit to the binary collision scaling limit, as expected, but instead it saturates and perhaps decreases at transverse momenta above 2 GeV/c.

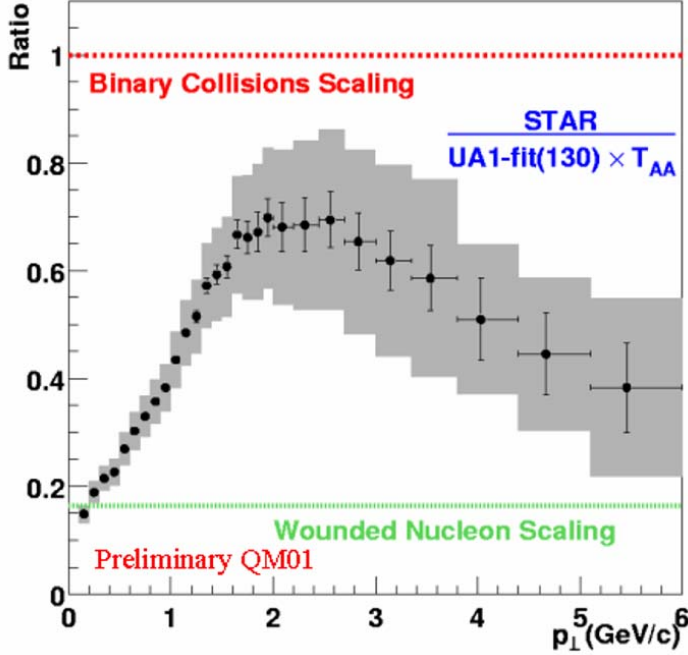


Figure 13: The yield of high  $p_T$  particles, at mid-rapidity, does not look like a simple binary scaling of proton-proton collisions. This may be evidence for radiative parton energy loss or other energy loss mechanisms due to the high gluon densities in the initial state.

The PHENIX collaboration has seen a similar phenomenon in their charged hadron data<sup>26</sup> at  $\sqrt{s} = 130$  GeV. They plot the yield of charged hadrons in central collisions (scaled per binary collision) compared to the yield of charged hadrons in peripheral collisions (scaled per binary collision) and show that it is suppressed at high  $p_T$ . They have also investigated the neutral  $\pi^0$  production yield. The data are shown in Figure 14 as a ratio  $R_{AA}$  where:

$$R_{AA} = \frac{\text{Yield}_{\text{central}} / \langle N_{\text{binary}} \rangle_{\text{central}}}{\text{Yield}_{pp}} \quad (4)$$

The figure suggests that the  $\pi^0$  data are even more suppressed at high  $p_T$  than the charged particle data shown in Figure 13.

Figure 14 also shows  $\pi^0$  data taken by the WA98 collaboration<sup>27,28</sup> at  $\sqrt{s} = 17.3$  GeV. The striking feature of the WA98 data is that it is not suppressed and it climbs to the binary collision scaling limit and even surpasses the limit. Presumably, the reason why the CERN data rises above 1.0 is that the Cronin effect comes into play and multiple

scattering in the initial state causes the incoming partons to have a modest  $p_T$  kick and this distorts the spectrum. The Cronin effect should also be at work in the RHIC data, trying to increase the ratio above 1.0, and so the WA98 data underscores the fact that the RHIC data is highly suppressed.

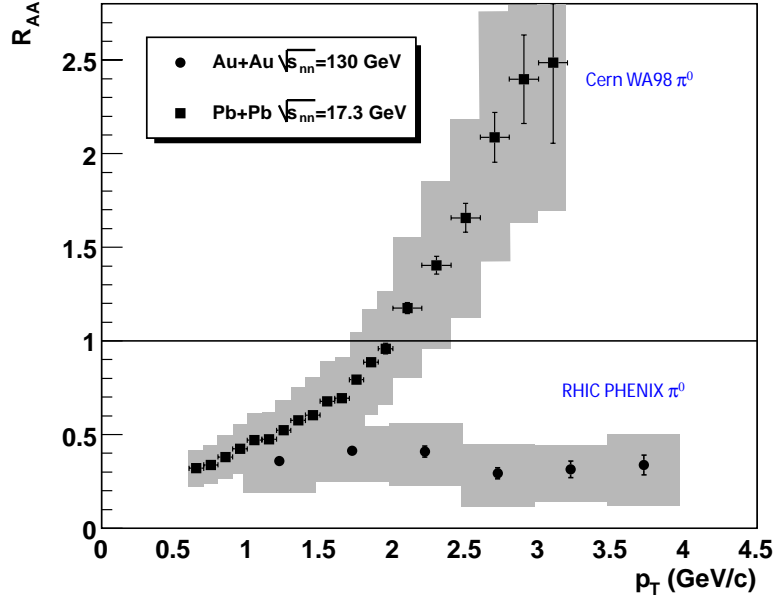


Figure 14: The PHENIX collaboration has measured the relative yield of charged and neutral particles at RHIC. The WA98 collaboration has made similar measurements at the CERN SPS. They are very different. The RHIC data are highly suppressed, perhaps by radiative parton energy loss mechanisms.

One possible explanation for the suppression effect is that a new energy loss mechanism is coming into play for the partons as they traverse the hot dense matter that is created in a nucleus-nucleus collision. Wang<sup>29</sup> has studied the data and he has successfully described the RHIC results using a parameterization of the Cronin effect, nuclear shadowing, and radiative parton energy loss. He estimates that the average parton  $dE/dx$  rate in Au-Au at RHIC energies is approximately 0.25 GeV/fm; but this effective value has been diluted by the rapid expansion of the fireball and he estimates that the rate of energy loss in a static system with a gluon density appropriate for the initial stages of the expanding system would be 12 GeV/fm. This is about 40 times higher than the rate of energy loss in cold, static, nuclear matter (0.3 GeV/fm), and since parton energy loss is proportional to gluon density, this suggests that the gluon density in the initial stages of a Au-Au collision is 40 times higher than in cold nuclear matter.

Finally, the PHENIX collaboration has measured the Bjorken energy density in Au-Au collisions at RHIC<sup>30</sup>. They use a large electromagnetic calorimeter to measure the total transverse energy in each collision. Then they apply the Bjorken formula for thermalized energy density to the top 2% most central collisions. Using a characteristic time of 1 fm/c, they find that Bjorken energy density is 4.6 GeV/fm<sup>3</sup>. This is a factor of 1.6 larger than at CERN energies ( $\sqrt{s} = 17.3$  GeV) and 30 times higher than in cold nuclear matter.



## Conclusions:

RHIC data are not what we had expected. Attempts to describe the data by extrapolating low energy cross-sections and low energy dynamics appear to be wrong, or incomplete. The best cascade model predictions at RHIC are made by HiJing and it has a lot of input from perturbative QCD and very little input from soft physics.

The initial state is very important. The Lorentz contraction of the incoming nucleus and the running of the coupling constant leads to gluon saturation. This effect suppresses the large multiplicity of particles that we expected based on simple  $\sqrt{s}$  scaling of low-energy data.

The initial state is also very dense. The energy density is high and the gluon density is high; both are 30 or 40 times higher than found in cold nuclear matter. The high value for the gluon density may cause unusually high radiative parton energy loss at high  $p_T$  and this could explain the suppression of elliptic flow at high  $p_T$ . The initial state also allows multiple scattering and the Cronin effect which are important in a complete description of the high  $p_T$  suppression of particle yields at RHIC.

RHIC and CERN data are different. Elliptic flow measurements at RHIC are in good agreement with the predictions of models based on hydrodynamics. This is a surprise because hydro models assume thermodynamic equilibrium and thermodynamic equilibrium is not a good description of CERN results, but yet the elliptic flow data suggest that RHIC collisions evolve very rapidly towards thermal equilibrium. In addition, the radial flow expansion velocities at RHIC are large; 55% of the speed of light. The RHIC and CERN data also differ by a factor of 1.5 to 2 in energy density, and the initial gluon densities are very different as can be seen by the dramatic suppression of high  $p_T$  particle yields at RHIC. The suppression is not seen in the CERN data.

Have we seen a new state of matter? It is hard to say; but the data do suggest that we seen a very unusual state of matter at RHIC.

---

<sup>1</sup> F. Karsch, hep-lat/0106019, hep-ph/0103314, and Nucl. Phys. **A698**, 199 (2002).

<sup>2</sup> <http://www.star.bnl.gov> and NIM A, RHIC Special Volume, in press.

<sup>3</sup> <http://www.phenix.bnl.gov> and NIM A, RHIC Special Volume, in press.

<sup>4</sup> <http://www.rhic.bnl.gov/brahms>

<sup>5</sup> <http://www.phobos.bnl.gov> and NIM A, RHIC Special Volume, in press.

<sup>6</sup> H. Wieman *et al.*, IEEE Trans. Nuc. Sci. **44**, 671 (1997) and J. Thomas, *et al.*, Nucl. Instrum. & Meth. **A478**, 166 (2002). See also: <http://www.star.bnl.gov> => Group Documents => TPC => Hardware.

<sup>7</sup> C. Adler, A. Denisov, E. Garcia, M. Murray, H. Strobele, and S. White, Nucl. Instrum. & Meth. **A470**, 488 (2001).

<sup>8</sup> B.B. Back *et al.*, Phys. Rev. Lett. **85**, 3100 (2000) and nucl-ex/0007036.

<sup>9</sup> B.B. Back *et al.*, Phys. Rev. C, in press, and nucl-ex/0201005.

<sup>10</sup> X.N. Wang and M. Gyulassy, Phys. Rev. Lett. **86**, 3496 (2001) and nucl-th/0008014.

<sup>11</sup> I.G. Bearden *et al.*, Phys. Lett. **B523**, 227 (2001) and nucl-ex/0108016.

<sup>12</sup> S.A. Bass *et al.*, Prog. Part. Nucl. Phys. **41**, 255 (1998) and nucl-th/9803035.

<sup>13</sup> B. Zhang, C.M. Ko, B.A. Li, and Z. Lin, Phys. Rev. C **61**, 067901 (2001) and nucl-th/9907017.

<sup>14</sup> I.G. Bearden *et al.*, Phys. Rev. Lett. **87**, 112305 (2001).

- 
- <sup>15</sup> D. Kharzeev and M. Nardi, Phys.Lett. **B507**, 121 (2001) and nucl-th/0012025.
- <sup>16</sup> B.B. Back *et al.*, Phys.Rev. **C65**, 031901 (2002) and nucl-ex/0105011.
- <sup>17</sup> D. Kharzeev and E. Levin, Phys.Lett. **B523**, 79 (2001) and nucl-th/0108006.
- <sup>18</sup> N. Xu Nucl. Phys. A 610, 175c (1996).
- <sup>19</sup> N. Xu and M. Kaneta, Nucl.Phys. **A698**, 306 (2002) and nucl-ex 0104021.
- <sup>20</sup> K.H. Ackermann *et al.*, Phys. Rev. Lett. **86**, 402 (2001) and nucl-ex/0009011.
- <sup>21</sup> C. Adler *et al.*, Phys. Rev. Lett. **87**, 182301 (2001) and nucl-ex/0107003.
- <sup>22</sup> C. Adler *et al.*, submitted to Phys. Rev. Lett. (2002) and nucl-ex/0206011.
- <sup>23</sup> J.C. Dunlop, Nucl. Phys. **A698**, 515 (2002).
- <sup>24</sup> Gyulassy, Vitev, and Wang, Phys. Rev. Lett. **86**, 2537 (2001) and nucl-th/ 0012092.
- <sup>25</sup> A. Bialas, M. Bleszynski, and W. Czyz, Nucl. Phys. **B111** (1976) 461.
- <sup>26</sup> K. Adcox *et al.*, Phys. Rev. Lett. **88**, 022301 (2002) and nucl-ex/0109003.
- <sup>27</sup> K. Reygers *et al.*, nucl-ex/0202018.
- <sup>28</sup> M.M. Aggarwal *et al.*, Eur. Phys. J. **C23**, 225 (2002) and nucl-ex/0108006.
- <sup>29</sup> X.N. Wang hep-ph/0111404.
- <sup>30</sup> K. Adcox *et al.*, Phys.Rev.Lett. **87**, 052301 (2001) and nucl-ex/0104015.